X-ray thin-film measurement techniques

V.   X-ray reflectivity measurement

Miho Yasaka*

1.   Introduction

This is the fifth article in the series of X-ray thin-film measurement techniques. The second, third and forth articles of this series, previously published in the Rigaku Journal, describe out-of-plane, high-resolution and in-plane XRD measurements to obtain crystallographic information on crystal size, lattice strain and orientation relationship of a thin-film material. These measurements have been based on the premise of a crystalline thin film. On the other hand, the X-ray reflectivity (XRR) measurement is not a technique to evaluate diffraction phenomenon. The XRR measurement technique described in this article is used to analyze X-ray reflection intensity curves from grazing incident X-ray beam to determine thin-film parameters including thickness, density, and surface or interface roughness. This article will provide an overview of the principles of X-ray reflectivity, measurement procedures, and analysis methods. It also discusses the procedural flow from measurement to analysis, as well as precautions.

2.   X-ray reflectivity measurement
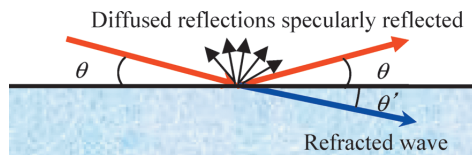
The X-ray reflectivity method has the following characteristics:

A)   It can be used to study a single-crystalline, polycrystalline or amorphous material.

B)   It can be used to evaluate surface roughness and interface width (arising from roughness and interdiffusion) nondestructively.

C)   It can be used to study an opaque film under visible light.

D)   It can be used to determine the layer structure of a multilayer or single-layer film.

E)   It can be used to measure film thickness from several to 1000 nm.

2.1.   The phenomenon of sample surfaces at grazing-angle incidence
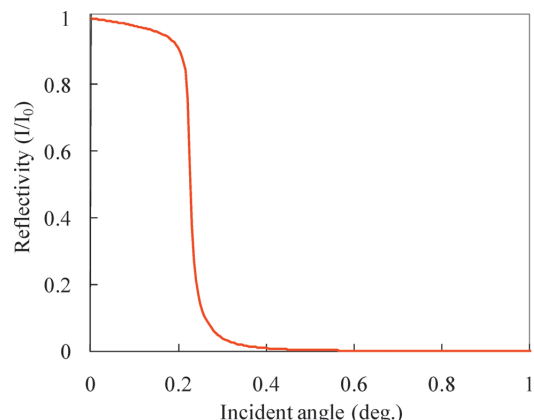
When electromagnetic waves including visible wavelength are incident onto a sample surface, these electromagnetic waves are reflected off it. The incident electromagnetic waves generate a specularly reflected wave, a refracted wave a diffused reflections, as shown in Fig. 1.

In the case of X-rays, which are incident

Fig. 1.   Reflection and refraction of X-rays on material surface.

electromagnetic waves, the refractive index of a material is slightly less than 1. Therefore, the X-rays undergo total reflection when incident on a flat surface of a material at a grazing angle is smaller than the critical angle for total reflection (θ_c). Thus X-ray reflectivity is related to the values of refractive index and X-ray wavelength. It should be noted that Cu-Kα X-rays is used throughout this article.

Fig. 2.   Reflectivity curve of Si.

Figure 2 shows a calculated X-ray reflectivity curve for bulk Si and Figure 3 shows the X-ray optics for the cases of the incident angles smaller, equal to, and greater than the critical angle for total reflection, θ_c. As shown in Fig. 2, when an X-ray beam is impinged at a grazing angle on to an ideal flat surface of a material, total reflection occurs at below the incident angle θ_c, and the incident X-rays do not penetrate into the material. X-ray reflectivity decreases rapidly with increasing incident angle, θ above θ_c. The ratio of specularly reflected X-rays decreases proportionally to θ^4.

* Application Laboratory, Rigaku Corporation.

A) Incident angle < Total reflection critical angle
All incident X-rays are reflected.

B) Incident angle = Total reflection critical angle
Incident X-rays propagate along the sample surface.

C) Incident angle > Total reflection critical angle
Incident X-rays penetrate into the material by refraction
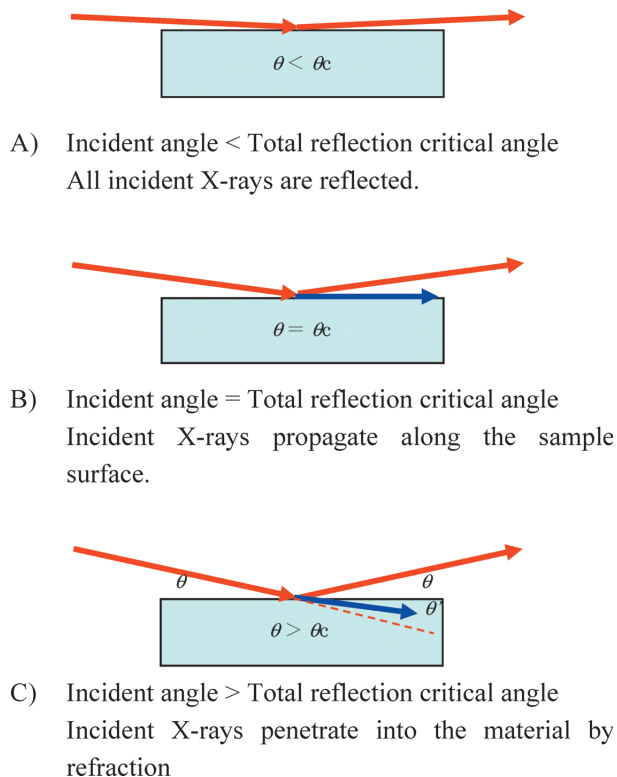
Fig. 3. Reflection and refraction of X-rays at material surface with the changes in the grazing angle.

2.2. Information provided by an X-ray reflectivity measurement

The X-ray optics for an X-ray beam onto a flat surface of material at grazing angles has been described in the previous section. In this section, the analysis of the resulting X-ray reflectivity curve to obtain information on the structural parameters of a thin film is described.

2.2.1. Film thickness

Changes in reflected intensity when a substrate made of an ideal material is laminated uniformly with a substance having a different electron density are described below. The observed scattering X-rays are the sum of individual electron scatterings. The intensity of X-ray reflectivity is calculated from each layer which is constructed from elemental species and filling rate of
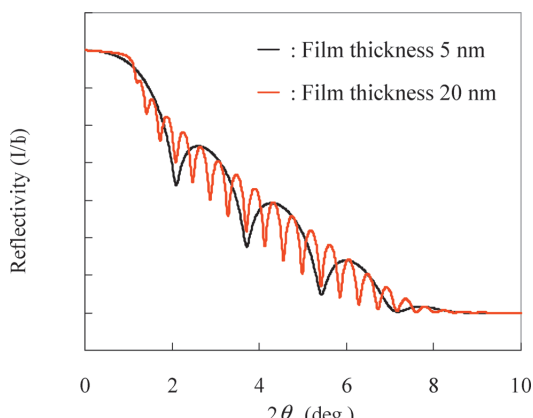
Fig. 4. Reflectivity of Au film on Si substrate.

space. Section 5 will describe total reflection and refraction in more detail. Figure 4 shows the X-ray reflectivity curve of an Au film deposited on a Si substrate. Generally, the Y-axis of X-raw reflectivity curve is shown in a logarithmic scale of the normalized intensity of I/I_0. A logarithmic scale is used because of the wide dynamic range of X-ray reflectivity intensity.

Interference occurs between the X-rays reflected from the surface of the Au film and the interface between the Au film and the Si substrate. As shown in Fig. 4, the reflectivity profile shows oscillations caused by this X-ray interference. These oscillations were first observed in 1931 by Kiessing and is called Kiessing fringes[1]. The oscillation depends on the film thickness, and the thicker film, the shorter period of the oscillations.

2.2.2. Density

The effects of thin-film density on an X-ray reflectivity curve are described below. Figure 5 shows the reflectivity curves of three 20 nm thick films with different densities deposited on Si substrates. The Au, Cu and SiO$_2$ films in Fig. 5 are used as examples for the cases of heavy, medium and light density materials, respectively.
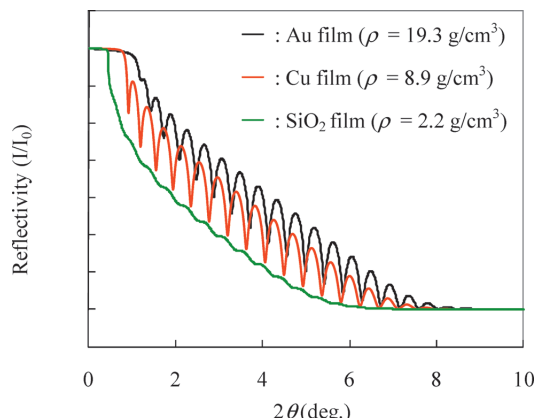
Fig. 5. X-ray reflectivity curves of Au, Cu and SiO$_2$ film on Si substrates (film thickness is 20 nm).
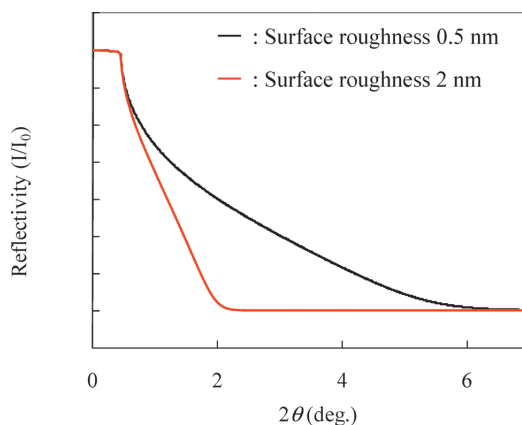
The results indicated that the amplitude of the oscillation and the critical angle for total reflection provide information on the density of films. The amplitude of the oscillation depends on the difference between the densities of the film and its substrate, the large the difference in the film density, the higher the amplitude of the oscillation.

2.2.3. Surface or interface roughness
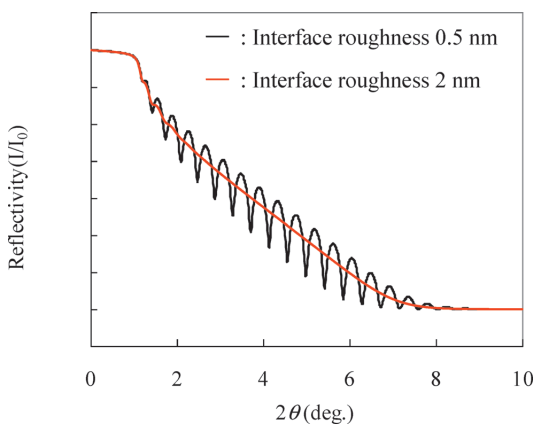
Figure 6 shows the reflectivity curves for a Si substrate with two different values of surface roughness.

The results shown in Fig. 6 indicate that reflected X-rays decrease more rapidly with a larger surface roughness. In other words, the larger the roughness of a film, the faster the decay rate of X-ray reflectivity.

On the other hand, Figure 7 shows the results of measurement for two types of substrates with different values of interface roughness. The results indicate that amplitude of the oscillation decreases with increasing
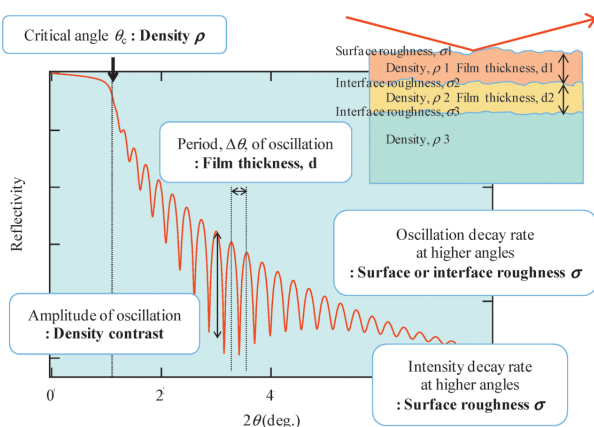
Fig. 6. X-ray reflectivity curves of Si substrates with two different values of surface roughness.

Fig. 7. X-ray reflectivity of Si substrate differences with interface roughness (Film thickness is 20 nm).

interface roughness. The term "interface roughness" includes that physical uneven interface and transitional boundary layer which continually changes in density. In both cases, interface roughness is recognized to a continuous variation of electric density along the thickness direction.

Figure 8 shows the summaries of the effect of film thickness, density, roughness of surface and interface on the X-ray reflectivity curve of a thin film deposited on a Si substrate.

Therefore, the X-ray reflectivity technique is a method for determining the layer structure of a thin film. The principles of X-ray reflectivity method will be described in section 5 in greater detail.
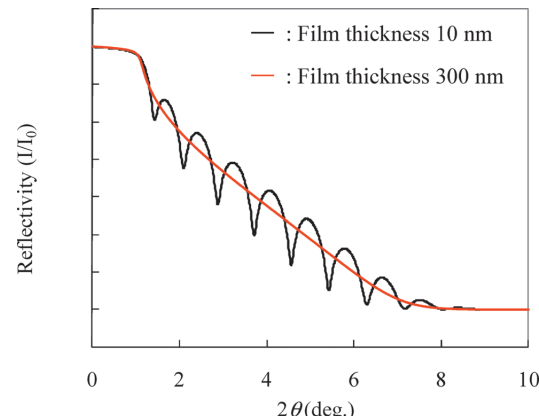
3. Useful methods and practices in X-ray reflectivity measurement

An accurate X-ray reflectivity curve is defined by clear appearances of the total reflection critical angle, the period and the amplitudes of the oscillation. It is necessary to obtain precise information so that appropriate X-ray optics depending on the film thickness and sample size are used. In addition, when an X-ray beam is incident on the sample at a grazing angle, a strict having adjustment is necessary.

3.1. Selecting incident optics

The X-ray reflectivity measurements must accurately measure a wide range of intensities measured at grazing X-ray incident angles. For grazing X-ray incidence, the use of a well-collimated incident X-ray beam is important. Conventional X-ray optics use narrow slits to collimate the incident X-ray beam. The intensity of the incident X-ray beam is thus very weak, and X-ray reflected curve with a wide dynamic range of intensity is difficult to obtain. Recently, an X-ray optical system equipped with a parabolic multilayer mirror and an incident-beam monochrometer has been used to produce a high-brightness and parallel incident X-ray beam.

The angular divergence of an incident X-ray beam can be controlled by incident X-ray optical systems. Therefore, X-ray optics must be selected on the basis of film thickness. Nowadays, to obtain a high-resolution and parallel incident X-ray beam, a parabolic multilayer mirror and an incident monochrometer are commonly used. Two X-ray reflectivity curves are compared using the X-ray optics system with a multilayer mirror, which gives the highest intensity among all incident X-ray optics. The multilayer mirror produces a parallel incident beam with a vertical divergence of around 0.04°. Figure 9 shows the X-ray reflectivity curves for two Au films with different thicknesses deposited on Si substrates.

Fig. 8. Information provided by X-ray reflectivity profile.

Fig. 9. Reflectivity of Au films on Si substrates (film thicknesses are 10 and 30 nm).

For the 300 nm thick film, oscillations of X-ray reflectivity cannot be observed using the optics system with a multilayer mirror. This is because the period of the oscillation changes depending on film thickness. With a larger film thickness, the period of the oscillation is smaller, and the resolution of the X-ray optics used for measuring X-ray reflectivity must be increased. Table 1 provides an overview of the optics used in reflectivity measurement and guidelines for film thickness measurement.

Table 1. Overview of optics used in a reflectivity measurement and guide for film thickness measurement.

Monochrometer	Multilayer mirror	Ge(220) 2-bounce	Ge(220) 4-bounce
Relative intensity (Reference estimation)	**200**	**10**	**1**
Resolution (Angular divergence)	up to 0.04°	up to 0.02°	up to 0.003°
Wavelength monochromaticity	$K\alpha_1 + K\alpha_2$ ($+K\beta$)	$K\alpha_1$	Part of $K\alpha_1$
Applicable film thickness	**0.5 to 100 nm**	**50 to 200 nm**	**200 nm or greater**

3.2. Relationship between incident angle and irradiated width

For a reflectivity measurement at a low-angle range $2\theta=0°$, the incident X-ray beam impinges onto a large area of the sample surface, even when a narrow incident slit is used. The length of the incident X-ray beam χ projected onto the sample surface can be calculated as follows:

$$x = \frac{W}{\sin \alpha} \tag{1}$$

where α is the angle of the incident X-ray beam W is the width of the incident beam slit. For example, in the case of an angle of incident X-ray of 0.2° and the width of the incident beam slit of 0.05 mm, the length of the incident X-ray beam projected onto the sample surface is calculated to be 15 mm. The spread of the incident beam is large when the incident angle is at and below the critical angle, the incident beam can spill over the sample surface. In this case, the critical angle, surface and internal roughness cannot be determined with a high degree of accuracy.

In addition, the irradiated X-ray beam also spreads along the horizontal direction. The irradiated width in the vertical direction is dependent on the height-limiting slit. However, the irradiated width should be approximately one-and-a-half times the height of the height limiting slit.

3.3. Sample alignment
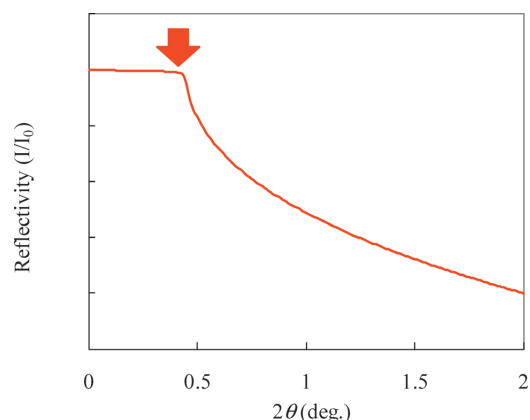
In the sample alignment process, the first step is to align the sample surface to be parallel to the incident X-ray beam (i.e., the direct beam), and an adjustment of the sample lengthwise axis (i.e., the Z axis) so that beam widths are divided into halves.

1. Set the 2θ axis to 0° to detect the incident X-ray beam directly.
2. Set the sample and retract the Z axis to the rear to avoid blocking the incident X-ray beam. Check intensity in this geometry.
3. Scan and set the Z axis at which intensity is half the intensity measured in step 2.
4. Scan the sample rotation axis (the ω axis) and adjust the alignment incident X-ray beam to obtain a maximum intensity.
5. Repeat the scans of both the Z and the ω axes for two or three times to make sure these axes and the sample surface are properly aligned.

After the alignment, the sample surface and incident X-ray beam are essentially parallel.

In the next step for a sample alignment, the incident X-ray beam is adjusted strictly in the total reflection range. The total reflection phenomenon occurs when the incident X-ray beam and the reflected X-ray beam have the same angle with respect to the sample surface. The total reflection phenomenon is highly sensitive to a change in intensity, which is accompanied by the incident X-ray angle, as shown in Fig. 2. Therefore, the angular position of the 2θ axis is set in the total reflection range (approximately 0.45° for Si), and multiple axes are aligned as follows:

1. Match the zero position of the 2θ axis and the zero position of the w axis obtained in the previous halving adjustment, and perform the reflectivity measurement by a $2q/w$ scan.
2. In this case, the total reflection occurs in the range near 0.2° to 0.45° on the $2\theta/\omega$ axis as shown in Fig. 10. Here, the halving adjustment with total reflection performs at 0.4° slightly lower than the critical angle.
3. Set $2\theta/\omega$ to 0.3° and scan the ω axis. The total reflection is observed when the incident X-ray beam and the reflected X-ray beam have the same angle with respect to the sample surface. At the peak angle position, the w axis is approximately half of the position on the 2θ axis.

Fig. 10. X-ray reflectivity measurement after halving adjustment.

4. Set the *w* axis at the peak position on 3.
5. Scan a sample swing axis (*c*, *Rx* or *Ry* axes).
6. Set the swing axis at the peak position on 5.
7. Repeat steps 3 to 6 until the peak positions on the *w* and the swing axes agree with those in the previous scan.

The two types of halving adjustments described above can be done using an appropriate X-ray reflectivity curve.

To ensure a precise X-ray incidence angle also requires various procedures for an accurate sample alignment. To facilitate these complex procedures, the software enabling easy acquisition of an appropriate reflectivity curve has been developed, recently. This software is equipped with an innovative function which makes the measurements under the conditions determined based on the sample width and height, film thickness, optics, etc.

3.4. Precaution attributable to sample

The preceding paragraph indicated that the incident optics and the height limiting slit size are dependent on the film thickness and the sample width. The precautions attributable to a sample are described below.

Rough sample surfaces may keep reflectivity profiles from exhibiting oscillations clearly because of diffused reflections. The reason is that diffused reflections are observed through the receiving slit. Diffused reflections should be removed so that high angular resolution capability can be achieved. In this case, depending on the extent of the roughness, using a narrow receiving slit and an analyzer crystal in the receiving optics may help to observe clearer oscillations.

If the sample is bent or corrugated, total reflection intensity may be stronger or weaker than that of the incident X-ray beam, as shown in Fig. 11(a), (b).
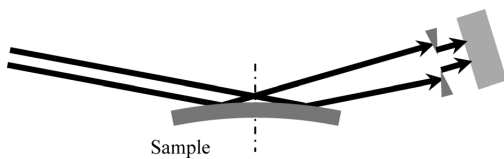
Fig. 11(a). Effects when sample is bent convexly.
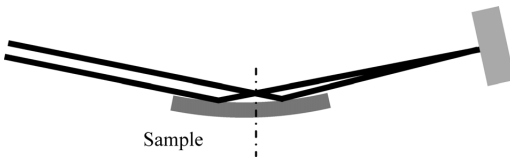
Fig. 11(b). Effects when sample is bent concavely.

If the sample is bent convexly, X-ray beams reflected from the sample will diverge. Some of the divergent intensities are shielded by the receiving slit resulting in a lowering the measured intensity. When the sample is concavely bent, the X-ray beam reflected from the sample converges, including the original divergent component in the incident X-ray beam, potentially resulting in a higher measured intensity. If the sample is not bent uniformly but is corrugated, both of the effects above occur simultaneously. If the sample is bent as above, a slightly larger receiving slit is recommended to detect all total reflection X-rays. A slightly larger high-limit slit is also recommended to obtain a more intense X-ray reflectivity curve for thin film analysis.

4. X-ray reflectivity measurement

Following selective optics and sample alignment perform reflectivity measurement, X-ray reflectivity measurement is based on the angles of ω and 2θ, which were obtained from the sample alignment, and each movement is scanned in the speed of $2:1$ (i.e., the $2\theta/\omega$ scan).

The scanning range is measured from below the critical angle to the angle where the measured reflection intensity reaches the level of the background. Generally, the scanning range is from $2\theta = 0.1 \sim 0.2°$ to $4 \sim 12°$.

The sampling width is applied to width in which profile shape near the critical angle or the oscillation in the reflection intensity is clearly observed without being squashed ($0.001°$ to $0.01°$). It is suitable to approximately 1/5 to 1/7 of the minimum period of the oscillation.

Scanning speed is set at the speed that statistical fluctuations can be suppressed to levels permitting a clear observation of the oscillation in the reflection intensities, clear of noise (e.g., $0.01°$ to $2°/\text{min.}$).

5. Reflectivity Analysis Method

The principles of the X-ray reflectivity method for determining film density, film thickness, and surface and interface roughness of a thin-film sample from the measured X-ray reflectivity curve are described below.

5.1. Total reflection and refractive index for X-Rays

The X-ray refractive index of a substance is slightly less than 1. If an X-ray beam strikes a substance with a flat surface at an incident angle equal to or less than the critical angle for total reflection, θ_c, and total reflection will occur as described in Section 2.1. The refractive index n of a material for X-rays can be calculated using the following equations:

$$n = 1 - \delta - i\beta \qquad (2)$$

$$\delta = \left(\frac{r_e \lambda^2}{2\pi}\right) N_0 \rho \sum_i x_i(Z_i + f_i') \bigg/ \sum_i x_i M_i \qquad (3)$$

$$\beta = \left(\frac{r_e \lambda^2}{2\pi}\right) N_0 \rho \sum_i x_i(Z_i + f_i'') \bigg/ \sum_i x_i M_i \qquad (4)$$

r_e: Classical radius of an electron ($2.818 \times 10^{-9}\,\text{m}$)
N_0: Avogadro number
λ: X-ray wavelength
ρ: Density (g/cm^3)

z_i: Atomic number of the i-th atom
M_i: Atomic weight of the i-th atom
x_i: Atomic ratio (molar ratio) of the i-th atom
f_i', f_i'':   Atomic scattering factors of the i-th atom
       (anomalous dispersion term).

As shown in Eq. (2), the refractive index is expressed as a complex number. The value of the parameter δ in the formula is ranging from 10^{-5} to 10^{-6} for X-rays with wavelength approximately 1 Å. As shown in Eq. (3), the value of δ depends on the X-ray wavelength and the density and composition of the material. The parameter β is related to X-ray absorption, expressed by the linear absorption coefficient μ as shown in the following formula:

$$\beta = \lambda \mu / 4\pi \qquad (5)$$

The critical angle θ_c for total reflection is given by the following formula:

$$\theta_c = \sqrt{2\delta} \qquad (6)$$

Thus, the density of the surface film can be obtained from the critical angle for total reflection, θ_c. As shown in Eq. (2), the refractive index of material depends on the X-ray wavelength and the density of material. When the X-ray wavelength is longer or the density of the material is greater the value of θ_c is larger. The θ_c is usually 0.2 deg to 0.5 deg.

5.2. Determining the thickness of a single-layer film

A periodical oscillation in intensity related to the thickness of a thin layer normally appears in an X-ray reflectivity curve. The thickness of a thin layer can be obtained by Fourier transformation of the extracted oscillation curve (see the right-hand curve in Fig. 12).
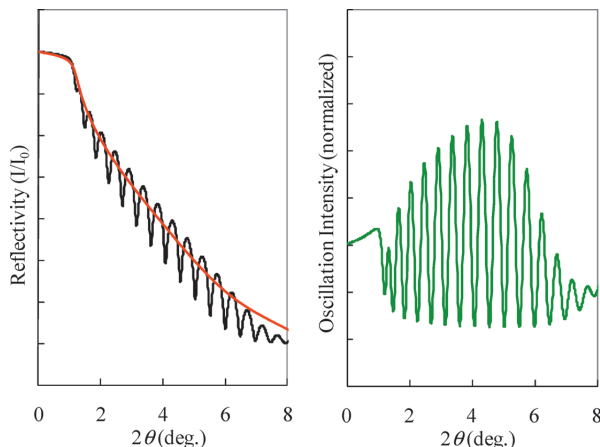
Fig. 12.   X-ray reflectivity curve of monolayer film (left) and the corresponding extracted oscillation curve (light).

The extracted oscillation curve is a function of the thickness d and refractive index δ of the layer. The oscillation is related to the following an equation:

$$\cos\left(4\pi d / \sqrt{\sin^2 \theta - 2\delta}\right) \qquad (7)$$
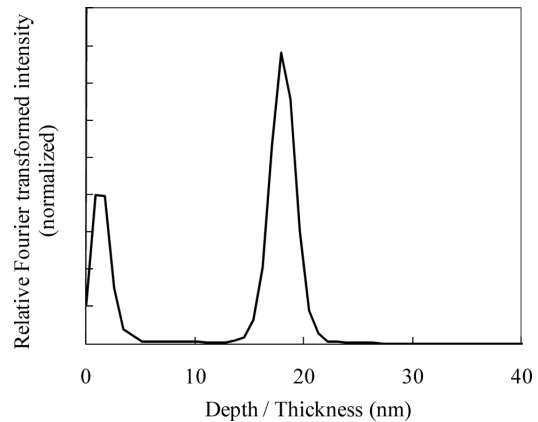
Fig. 13.   Profile after Fourier transformation.

The thickness can be estimated from the peak position of the profile of Fourier transformation plotted with a horizontal axis in the scale of $\lambda \sqrt{\sin^2 \theta - 2\delta}$ as shown in Fig. 13.

However, this method cannot be used to obtain the density, surface nor interface roughness of a multilayer film. Values of thickness, density, surface and interface roughness of a multilayer film can be obtained by a non-linear least-squares fitting as described below.

5.3. Theoretical calculation of X-ray reflectivity from multilayer films

X-ray reflection occurs at all interfaces in a multilayer film. The X-ray reflectivity of a multilayer film as a function of θ can be theoretically calculated using the recurrence Eq. (8)[2],[3].

In Eq. (8), the vacuum or gas phase on top of a film with n layers is regarded as the $j=1^{st}$ layer. Each layer in the multilayer film is numbered in sequence starting with $j=2$, and a substrate is considered as the $j=n+1$ layer. When the reflection coefficient at the interface between the jth and $(j+1)^{th}$ layers is defined as $R_{j,j+1}$, the value of $R_{j,j+1}$ can be calculated using the following recurrence formula:

$$R_{j,j+1} = \frac{R_{j+1,j+2} + F_{j,j+1}}{R_{j+1,j+2} \times F_{j,j+1} + 1} a_j^4 \qquad (8)$$

$$F_{j,j+1} = \frac{g_j - g_{j+1}}{g_j + g_{j+1}} \exp\left(\frac{-8\pi^2 g_i g_{j+1} \sigma_{j+1}^2}{\lambda^2}\right) \qquad (9)$$

$$a_j = \exp(-i\pi g_j d_j / \lambda) \qquad (10)$$

$$g_j = \sqrt{n_i^2 - \cos^2 \theta} \qquad (11)$$

The recurrence Eq. (8) together with Eqs. (9) to (11), can be used to calculate the values of $R_{j,j+1}$ first starting at the interface on top of the substrate, and then the next upper interface in sequence up to the surface layer. The X-ray reflectivity $I/I_0 = R_{1,2}$ is last calculated. Please note that the substance is assumed to be sufficiently thick that no reflectivity will occur from the bottom of the

6

5.4. Reflectivity analysis method of a multilayer film

Generally, an X-ray experimental reflectivity curve is compared to the theoretical curve calculated based on a layer structure model. The solution with optimal parameter values of thickness, density, and roughness of the interface in the multilayer film is obtained when the residual between the measured and calculated reflectivity data reaches a minimum.

Figure 14 shows an example of using the GlobalFit software in the Integrated Thin Film Analysis Software package for an X-ray reflectivity analysis. The GlobalFit software can simulate a reflectivity curve based on the created layer structure even without the need of measured data. In addition, this software can analyze a periodic multilayer film or layers with a density-depth distribution. Most of the common data analysis technique used to obtain values of layer parameters is the least-squares method. If the measured profile and the simulation result do not agree, it is not easy to obtain the optimum layer structure parameters, because the least-squares refinement can be trapped in a local minimum. To avoid the local minimum problem, two other optimization methods along with the conventional least-square methods are included in the Rigaku reflectivity analysis software package for the determination of optimum layer structure parameters. One of the methods is called "extended Fourier analysis", and the other is called "global optimization". These two optimization methods make it possible to perform an X-ray reflectivity analysis of a complex multilayer film efficiently.
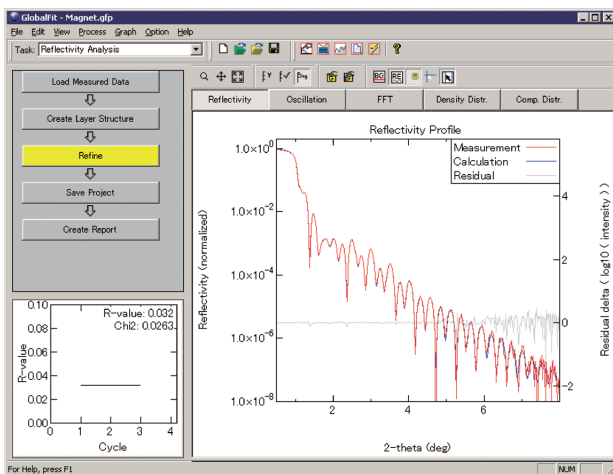
Fig. 14. Integrated Thin Film Analysis Software "GlobalFit" used for reflectivity analysis.

6. Examples of X-ray Reflectivity Analysis

This section discusses the analysis of measured data for a multilayer film with a complex layer structure. The sample used in this example is a magnetic Ta/NiFe film on a glass substrate. The nominal thickness for the Ta and the NiFe layers are 20 nm and 15 nm, respectively.
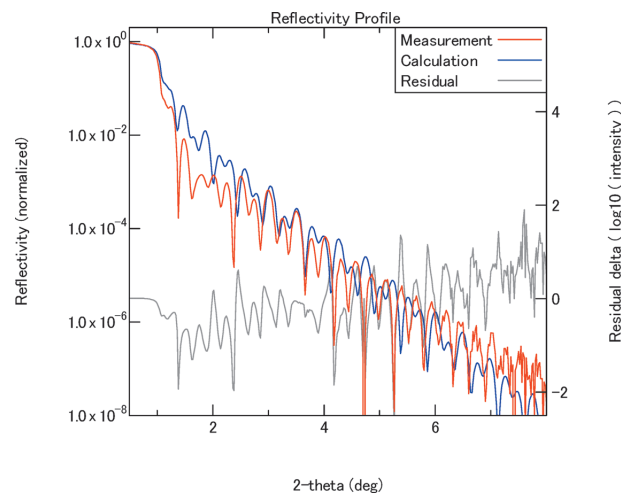
Fig. 15. Measured sand simulated reflectivity curves for a magnetic film (Ta(20 nm)/Ni(15 nm)/grass substrate).

Figure 15 shows the experimental data (the red curve) and the calculated simulation data (the blue curve) for the sample.

As shown in Fig. 15, the oscillations in the measured and simulated data do not match. Therefore, the thickness values for Ta and/or NiFe layers are probably slightly different from the true values. The "extended Fourier analysis" software was then used to optimize the initial value of the layer structure parameters specified initially to the actual sample structure. Figure 16 reveals that there is an additional exceedingly thin layer presented in the multilayer film.
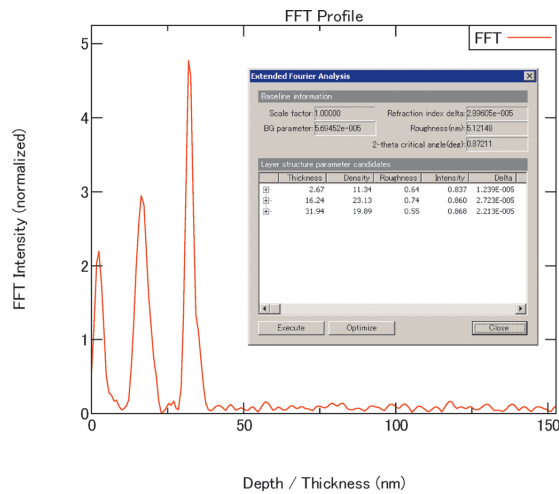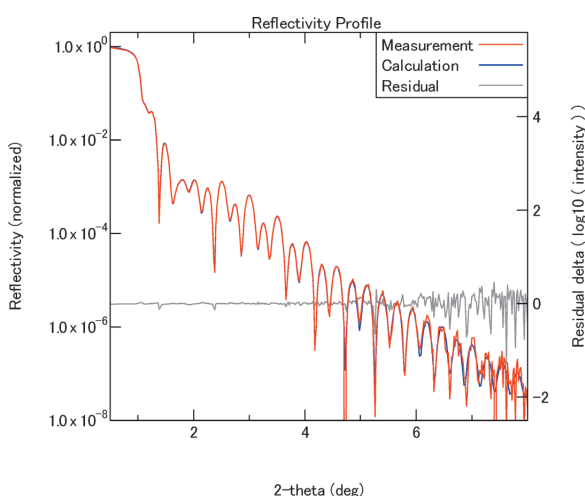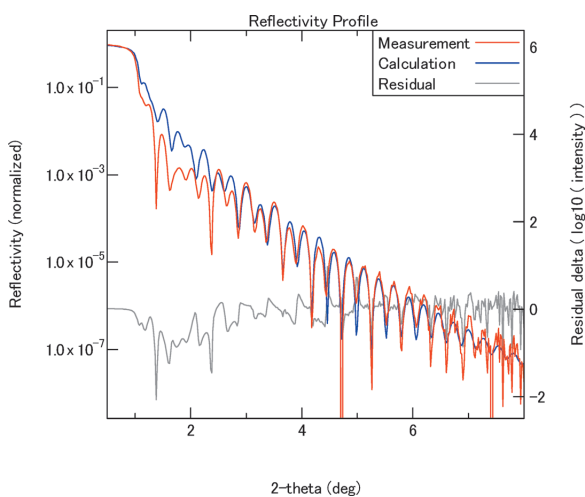
Fig. 16. The Fourier transform profile.
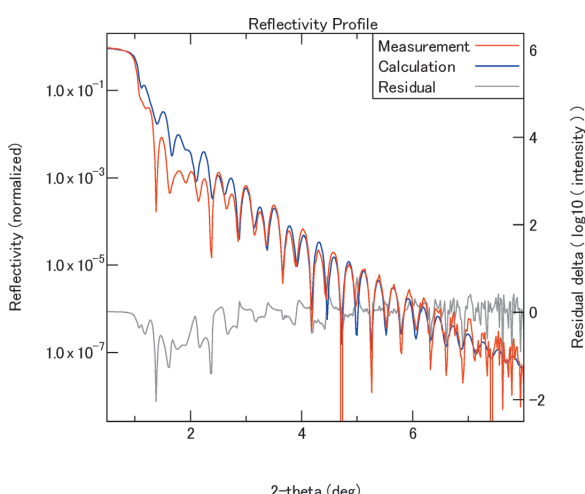
As shown in Fig. 16, from the result of the Fourier transform analysis, a thin layer approximately 2~3 nm thick should be presented in the film. However, the results of the Fourier analysis do not give information on the sequence of the layers among the depth direction. Therefore, the thin layer which is approximately 2~3 nm thick can be presented with one of the following three possibilities:

(1) The thin layer is presented on the surface of the Ta layer.

(2) The thin layer is presented at the interface between the Ta and the NiFe layers.

(3) The thin layer is presented at the interface between the NiFe layer and the glass substrate.

Fig. 17. The simulation results of the magnetic film.

1. The thin layer is presented on the surface of the Ta layer.
2. The thin layer is presented at the interface between the Ta and the NiFe layers.
3. The thin layer is presented at the interface between the NiFe layer and the glass substrate.

The thickness was first optimized based on the results of the Fourier analysis and X-ray reflectivity profile was then refined using the GlobalFit and the least-squares methods based on the layer structure of the above three possibilities: No. 1, 2 and 3. Figure 17 shows the analysis results for No. 1, 2 and 3.

Among the three figures in Fig. 17, possibility No. 1 gives the best match between the experimental and the calculated curves, suggesting that this thin layer, probably a tantalum oxide layer, is presented on the surface on the Ta layer. It should be noted that an XRD analysis of thin-film diffraction peaks obtained by out-of-plane and in-plane diffraction may be able to provide more structural information on this film including the thin tantalum oxide layer.

7.   Concluding remarks

The principles of the X-ray reflectivity method, measurement procedures, and data-analysis methods have been described. The X-ray reflectivity method is nondestructive and can be used for evaluating the layer structure, thickness, density, and surface or interface roughness of a multilayer film.

In recent years, a working group has been set up to share information and problem consciousness because of diversification of target samples and highly-developed and complicated analysis techniques[4]. Recently many articles on the applications of the X-ray reflectivity method have been published in the literature. For examples:

1. Articles of accurate thin-film analysis using the X-ray reflectivity method[5]–[7].
2. An article on a study of the coefficients of thermal expansion of thin films prepared under high temperatures[8].
3. Articles on the study of the flatness of "buried interface" and detections of reaction phases at interfaces[9],[10].
4. An article on the analysis of density and thickness of self-organized organic monomolecular film[11].
5. Articles on the analysis of organic layers of a film with density-depth distributions[12],[13].

In addition, the average density of a porous material obtained by the X-ray reflectivity method was used to evaluate the proportion of pore and the evaluation of layer structure[14]–[16].

The next review article of this series will be X-ray thin-film measurements using the small angle X-ray scattering (SAXS) method.

References

(1) H. Kiessig: *Ann. Phys.*, **10** (1931), 715–768.

(2) L. G. Parratt: *Phys. Rev.,* **95** (1954), 359–369.

(3) S. K. Sinha, E. B. Sirota and S. Garoff: *Phys. Rev*., **B38** (1988), 2297–2311.

(4) http://www.nims.go.jp/xray/ref/

(5) K. Omote and Y. Ito: *Hyomen Kagaku* (Japanese), **27** (2006), 642–648.

(6) A. Kurokawa, K. Odaka, T. Fujimoto and Y. Azuma: *Shinku* (*Jour. Vac. Soc. Jpn.*) (Japanese)*,* **50** (2007), 199–201.

(7) T. Fujimoto, S. Yamagishi, Y. Azuma, T. Taketsuji and T. Watanabe: *Hyomen Kagaku* (Japanese), **28** (2007), 494–499.

(8) K. Omote and Y. Ito: *Mater. Res. Soc. Symp. Proc.*, **875** (2005), O8.2.1.

(9) H. Ohta, T. Mizoguchi and Y. Ikuhara: *Material Integration* (Japanese)*,* **22** (2009), No. 9–10, 38–42.

(10) H. Shimizu, K. Kita, K. Kyuno and A. Toriumi: *Jpn. Jour. Appl. Phys.,* **44** (2005), 6131–6135.

(11) S. Kobayashi, T. Nishikawa, T. Takenobu, S. Mori, T. Shimoda, T. Mitani, H. Shimotani, N. Yoshimoto, S. Ogawa and Y. Iwasa: *Nature Materials,* **3** (2004), 317–322.

(12) T. Fukuyama, T. Kozawa, K. Okamoto, S. Tagawa, M. Irie, T. Mimura, T. Iwai, J. Onodera, I. Hirosawa, T. Koganesawa and K. Horie: *Jpn. Jour. Appl. Phys.,* **48** (2009), 06FC03-1–06FC03-3.

(13) T. Fukuyama, T. Kozawa, S. Tagawa, R. Takasu, H. Yukawa, M. Sato, J. Onodera, I. Hirosawa, T. Koganezawa and K. Horie: *Appl. Phys. Express,* **1** (2008), 065004-1–065004-3.

(14) Y. Ito: *Material Stage* (Japanese)*,* **8** (2004), 27–34.

(15) T. Suzuki, K. Omote, Y. Ito, I. Hirosawa, Y. Nakata, I. Sugiura, N. Shimizu and T. Nakamura: *Thin Solid Films*, **515** (2006), 2410–2414.

(16) Y. Ito: *Shinku* (*Jour. Vac. Soc. Jpn.*) (Japanese)*,* **49** (2006), 104–108.